Title

Paraventricular Thalamus Neuronal Ensembles Encode Early-life Adversity and Mediate the Consequent Sex-dependent Disruptions of Adult Reward Behaviors

Journal

bioRxiv, 5(05-14)

ISSN

2692-8205

Authors

Kooiker, Cassandra L
Birnie, Matthew T
Floriou-Servou, Amalia
et al.

Publication Date

2024-04-29

DOI

10.1101/2024.04.28.591547

Title:

Paraventricular Thalamus Neuronal Ensembles Encode Early-life Adversity and Mediate the Consequent Sex-dependent Disruptions of Adult Reward Behaviors

Cassandra L. Kooiker[1], Matthew T. Birnie[1,2], Amalia Floriou-Servou[1], Qinxin Ding[3], Neeraj Thiagarajan[3], Mason Hardy[1], Tallie Z. Baram[1,2,4]*

[1] Department of Anatomy/Neurobiology, University of California-Irvine, Irvine, CA, USA.
[2] Department of Pediatrics, University of California-Irvine, Irvine, CA, USA.
[3] School of Biological Sciences, University of California-Irvine, Irvine, CA, USA.
[4]Department of Neurology, University of California-Irvine, Irvine, CA, USA

* Corresponding author

Correspondence: tallie@uci.edu

Abstract

Early-life adversity increases risk for mental illnesses including depression and substance use disorders, disorders characterized by dysregulated reward behaviors. However, the mechanisms by which transient ELA enduringly impacts reward circuitries are not well understood. In mice, ELA leads to anhedonia-like behaviors in males and augmented motivation for palatable food and sex-reward cues in females. Here, the use of genetic tagging demonstrated robust, preferential, and sex-specific activation of the paraventricular nucleus of the thalamus (PVT) during ELA and a potentiated reactivation of these PVT neurons during a reward task in adult ELA mice. Chemogenetic manipulation of specific ensembles of PVT neurons engaged during ELA identified a role for the posterior PVT in ELA-induced aberrantly augmented reward behaviors in females. In contrast, anterior PVT neurons activated during ELA were required for the anhedonia-like behaviors in males. Thus, the PVT encodes adverse experiences early-in life, prior to the emergence of the hippocampal memory system, and contributes critically to the lasting, sex-modulated impacts of ELA on reward behaviors.

Introduction

Early-life adversity (ELA) such as abuse, poverty, or tumultuous environment impacts the lives of over 30% of children in the United States[1] In humans, studies have shown that ELA is significantly associated with an increased risk of affective disorders including depression, post-traumatic stress disorder PTSD, and substance use disorders[2-5], and these risks are modulated by sex. Imaging studies in humans have identified aberrant development of reward circuit connectivity, critical for emotion regulation, motivation and the experience of pleasure, following ELA[6-9].

Complementing human research, animal studies have been pivotal in demonstrating a causal relationship between ELA and disruptions of reward behaviors[10-15]. Such work has also been instrumental in unraveling the neurobiological mechanisms involved in the consequences of

adverse early adverse experiences. For examples, experimental model studies have shed light on how ELA alters subsequent responses to stress and how a transient ELA is converted into lasting outcomes via persistent changes in gene expression through epigenetic mechanisms[10,16-18]. Importantly, as in humans, the effects of ELA on adult motivated behaviors in rodents are modulated by sex and thus provide a platform to probe the mechanisms nature by which ELA provokes disruptions in reward behaviors. However, while significant progress in addressing these issues has been made, key questions have been unanswered: Where in the brain is ELA encoded? Do neuronal populations engaged by ELA also contribute to the disruption of adult reward behaviors? And what is the neurobiological basis for the profound sex-differences in these dysregulations?

Using combined genetic tagging and the expression of the immediate early gene cFos, we have previously described robust, almost exclusive activation of the paraventricular nucleus of the thalamus (PVT) during ELA (as well as during positive salient early life experiences) that takes place during the first postnatal week in the rodent[19,20]. Importantly, among all analyzed brain regions, activation of neurons within the PVT was the only region that distinguished ELA from standard rearing: in males, a larger number of PVT neurons were genetically tagged, and, in both sexes, a higher proportion of tagged cells expressed the receptor for the stress-sensitive peptide corticotropin releasing hormone (CRH) in ELA mice as compared to typically reared mice. These findings suggest the PVT may encode and hence potentially mediate the long-term behavioral consequences of ELA.

The PVT is an important component of limbic and emotional processing networks[21], contributing to the determination of cue salience by integrating information on internal states as well as the external environment, incorporating prior salient experiences[22,23,37]. The PVT interconnects with brain regions implicated in stress and aversive experiences, such as the extended amygdala,

brainstem, and the medial prefrontal cortex (mPFC) and also sends dense projections to the nucleus accumbens (NAc), a critical node of the reward circuit[24-27]. Via this unique connectivity, the PVT straddles competing motivational circuits to gate the expression of motivated behaviors and modulate responses to stress[28-33]. Notably, whereas the role of the PVT in incorporating past salient experiences into decisions involving motivated reward behavior in the adult has been established[34-37], it has remained unknown whether such past salient experiences can be as remote as those taking place neonatally. Further, the sex-specific roles of distinct domains of this heterogeneous structure in integrating prior experiences to influence reward behavior have remained unexplored. The current studies aimed to address these fundamental information gaps.

Results

Differential activation of PVT and its interconnected networks by early-life adversity versus typical neonatal experiences

We capitalized on the TRAP2 mouse system, which allows for permanent activity-dependent labeling of neurons active during a defined 24-36 hour time period[38], and generated ELA using the limited bedding and nesting (LBN) model established in our lab and widely adopted around the world[39,40]. The paradigm involves rearing pups for a week during an early sensitive developmental period (postnatal days [P]2-9) in a resource-scarce environment[14,39], which consistently induces sex-dependent changes in reward behavior when rodents reach adulthood[11,13,40]. We induced the TRAP2 system midway during the ELA epoch (P6), thereby inducing recombination in, or "TRAPing," neurons active on P6 and P7. Quantification of activated (TRAPed) PVT neurons showed that ELA led to a significantly augmented number of activated PVT neurons compared to standard rearing in males (**Fig.1A, B, E**), in accord with our prior finding[19]. In females, whereas the total number of activated cells was similar in ELA and control mice (**Fig. 1C-E**), a significantly larger proportion of PVT neurons active during ELA expressed the CRH receptor, CRFR1, as was also the case in males[19].

The PVT is a hub interconnected with several, sometimes competing, motivational circuits (e.g., threat vs. reward), and the connectivity of the PVT within these brain networks may be altered during ELA, potentially influencing the computations executed by the PVT to adjudicate motivation for adult reward behaviors. Therefore, we performed cross correlation analysis of the activation of neurons in the PVT and in other brain regions during ELA or standard rearing to determine if such correlations, a surrogate for network connectivity, might be influenced by ELA (**Fig. 1F, G**). We generated Pearson correlation coefficients for each pair of regions to identify co-activation in each mouse group and created correlation matrices using this information (**Supp. Fig. 1**). We then converted Pearson correlation coefficients to z-scores and determined the difference between these scores among rearing groups for each sex, taking into account the number of observations within each rearing group for each pair.

Cross-correlations among brain regions activated during ELA differed significantly from those during standard rearing and were further influenced by sex (**Fig. 1F, G**). In males, correlated expression of the TRAP reporter between the posterior PVT and basolateral amygdala (BLA) was significantly reduced in ELA-compared to control males (Z_{obs} = -1.99; **Fig. 1F**). In addition, activation in the BLA and prelimbic cortex was less correlated in ELA males compared with controls (Z_{obs} = -2.04; PrL). In females, we identified a robust increase in activation cross-correlation between the anterior PVT and lateral hypothalamus (LH) in the ELA group (Z_{obs} = 2.59) as well as a significantly stronger co-activation between the dorsal CA1 (dCA1) and dorsal dentate gyrus (dDG; Z_{obs} = 2.47; **Fig. 1G**). Together, these data suggest that, in addition to differential engagement of the PVT itself during ELA or control rearing, correlation of neuronal ensembles in salient components of networks involving the PVT were altered.

Reward-induced reactivation of early-life-engaged PVT neurons

The experiments described above show that PVT neuronal subsets are differentially activated by ELA and control rearing in a manner modulated by sex. To begin to assess whether PVT neurons

active during ELA may also contribute to the aberrant adult reward behaviors consequent to ELA, we tested for the activation of these same neurons in adults exposed to a reward. Specifically, after genetically tagging PVT neurons during ELA, we examined overall PVT activation as well as reactivation of early-life-engaged PVT neurons during an adult reward task. We exposed TRAP2 ELA and control mice (which had received tamoxifen on P6 to permanently visualize neurons activated early in life) to 1.5 hours of free access to palatable food. We then perfused them to analyze cFos expression as well as cFos co-expression with the TRAP reporter, an indicator of re-activation of neurons engaged early in life.

A significantly larger number of ELA-engaged PVT neurons were *reactivated* during the task in the ELA mice compared to reactivation by reward of PVT neurons in the standard rearing groups in both males (**Fig. 2A**) and females (**Fig. 2F**). The total number of neurons expressing cFos upon reward exposure was also significantly greater in ELA males and females compared to their respective control groups (**Fig. 2B, G**). While the overall number of early-life-engaged PVT neurons that are reactivated was greater in ELA males compared to controls, the fraction of TRAPed neurons reactivated during palatable food exposure did not differ between ELA and control males (**Fig. 2C**), likely because of the greater total number of TRAPed PVT neurons in ELA males. In contrast, in females, a larger proportion of ELA-TRAPed PVT neurons were reactivated in the ELA group compared to controls (**Fig. 2H**).

<u>Inhibition of early-life-engaged anterior PVT neurons normalizes reward behaviors in adult ELA males</u>

Exposure to ELA leads to sex-dependent, opposing disruptions of adult reward behaviors. Adult male ELA mice display an anhedonia-like phenotype, whereby they consume less of a palatable food and are less interested in a sex-cue[11,40,41]. In contrast, adult female rodents exhibit an augmented reward seeking phenotype relative to females reared in standard cages[42-44]. This dichotomy suggests that ELA is encoded and processed in a sex-dependent manner to influence behavior later in life. Within the heterogeneous PVT, the anterior and posterior PVT differ in cell

composition and connectivity, endowing them with both overlapping and discrete functions[45-48]. In view of this domain specificity within PVT, we chose to manipulate, using chemogenetics, the anterior and posterior PVT separately.

We determined whether inhibition of ELA-engaged anterior PVT neurons ameliorated the deficits in reward behaviors in adult ELA-males. We used Fos$^{2A\text{-}iCreER+/-}$::R26-LSL-Gi-DREADD mice that received tamoxifen on P6 (of ELA or standard rearing) to induce expression of the inhibitory designer receptor responsive to designer drug (DREADD) HA-hM4Di-pta-mCitrine only in neurons active from P6-P7, enabling chemogenetic inhibition of this neuronal population later in life. To limit chemoinhibition to PVT neurons only, we implanted cannulae in either the anterior PVT or posterior PVT and administered the DREADD ligand clozapine-N-oxide (CNO) via the cannulae (**Fig. 3A, Supp. Fig. 2**). Following infusion of CNO or vehicle, male mice underwent one of two reward tasks: palatable food consumption during one hour of free access or exploration of a sex cue[49,50]. Inhibition of ELA-engaged neurons in the anterior PVT in adult male ELA mice restored their palatable food consumption back to levels seen in typically reared mice (**Fig. 3B**) and also normalized their interest in a sex cue (**Fig. 3C**). By contrast, inhibition of early-life-engaged anterior PVT neurons had no effect in the control group in either task (**Fig. 3B, C)**. Notably, locomotion was not influenced by CNO or rearing in males, excluding off-target effects of CNO (**Supp. Fig. 3**).

In females, we determined whether inhibition of ELA-engaged anterior PVT neurons may ameliorate the aberrantly augmented reward behaviors in adult ELA-females using a similar approach. Selective inhibition of ELA-engaged neurons in the anterior PVT did not influence the augmented consumption of palatable food in adult ELA females (**Fig. 3E**). Surprisingly, this manipulation in control females increased their palatable food consumption to levels observed in the ELA group, suggesting that anterior PVT may act as a brake on palatable food consumption

in both sexes. Again, CNO did not influence locomotion in either female group, suggesting the absence of any off-target actions. (**Supp. Fig. 3**).

Together, these findings demonstrate the contribution of anterior PVT neurons activated during ELA to the resulting anhedonia-like phenotype in males, and further suggest that the mechanisms by which ELA influences anterior PVT neurons differ by sex.

Inhibition of early-life-engaged posterior PVT neurons normalizes reward behaviors in adult ELA females

The posterior PVT has been shown to be activated by adverse experiences in adults and to influence subsequent behaviors and responses to stress[18,29-31,34]. Therefore, we sought to determine if inhibition of posterior PVT neurons activated by ELA modulates the aberrant sex-dependent reward behaviors generated by ELA.

In ELA males, selective chemogenetic inhibition of posterior PVT neurons engaged by ELA had no effect on adult anhedonia-like behavior in the palatable food test (**Fig. 4B**), nor did it alter ELA male behavior in the sex cue preference task (**Fig. 4C**). Inhibition of early-life-engaged posterior PVT neurons in control males, however, decreased consumption, recapitulating the ELA phenotype (**Fig. 4B**).

The effect of selective chemogenetic inhibition of posterior PVT neurons activated early in life was highly sex-specific. In adult females, inhibition of these neurons had no influence on palatable food consumption in adult control females. In contrast, the same infusion into the posterior PVT of ELA females significantly reduced their augmented palatable food consumption, reversing the effect of ELA (**Fig. 4E**). These results support an important contribution of ELA-engaged neurons in the posterior PVT in mediating the aberrantly augmented reward behavior consequent to ELA in females, whereas in males, activity of posterior PVT cells engaged by salient early-life experiences may promote anhedonia-like behaviors.

Discussion

Here we demonstrate that specific populations of PVT neurons that are active during ELA contribute crucially and enduringly to disrupted reward behaviors in adults following ELA in a sex-dependent manner. Our principal discoveries are: 1) Patterns of PVT neuron co-activation with other salient brain regions are influenced by ELA in a sex dependent manner, perhaps contributing differentially to circuit maturation; 2) ELA augments activation of PVT neurons during a reward task, as well as increases the reactivation of early-life-engaged PVT neurons in a sex-dependent manner; 3) Distinct PVT domains contribute differentially to the disrupted reward behaviors in males and females, with unique contributions of the anterior vs. posterior PVT, which may provide insight into the discrete roles of these regions in motivated behaviors. Together the findings uncover the profound and complex role of PVT neuronal ensembles engaged very early in life in the execution adult reward behaviors.

Differential engagement of brain networks by salient emotional experiences in developing males and females

Our cross-correlation analyses revealed intriguing relationships among stress- and reward-related brain regions with known physical connectivity with the PVT. In males, we identified decreased correlated neuronal activity between the pPVT and basolateral amygdala (BLA) during ELA as compared to standard rearing. The BLA is vital to emotional processing and behaviors and acts to modulate emotional memory[51,52]. Projections from the PVT to the BLA are known to mediate reward and punishment learning and modulate anxiety-like behavior[53,54]. Decreased activity in this projection provoked by ELA could therefore interfere with motivated behavior later in life, providing a potential explanation for the anhedonia-like phenotype seen in males following ELA. In contrast, we found increased functional connectivity between the lateral hypothalamus (LH) and aPVT in females during ELA. The LH, most known for its roles in feeding behaviors, is a major source of input to the PVT[55,56]. Orexinergic projections from the LH to the PVT are known to regulate attribution of incentive salience to rewarding stimuli and cues that predict them[55]. Our

finding of increased LH-aPVT functional connectivity during ELA in females therefore suggests that ELA-induced plasticity of this projection may contribute to the binge-eating-like phenotype seen in ELA females.

Augmented activity and reactivation of PVT neurons in adult ELA mice during reward computations

We identified increased PVT activation, as measured by cFos expression, during an adult reward task in ELA groups of both sexes, as compared to control groups. This increased activation indicates that ELA has a lasting effect on the operations of the PVT, inducing hyperresponsiveness to reward. This effect was particularly prominent in the anterior PVT, which is crucial in signaling arousal[23,57]. Following ELA, the PVT may be signaling an altered state of arousal during reward behaviors, reflecting hyperarousal consequent to this remote stressor. Alternatively, with consideration of the PVT's role as an adjudicator of behavior during motivational conflict, ELA may shift the increase the weights of competing motivational input, increasing the computational burden on the PVT. This may be reflected as recruitment of a larger number of PVT neurons[36].

The increased reactivation of ELA-engaged PVT neurons during reward behaviors suggests that these neurons are persistently altered by ELA, rendering them more sensitive to reward exposure. Indeed, recent work from our group shows sex-dependent changes in gene expression at baseline and a very different translatomic response upon exposure to a palatable food reward in ELA mice as compared to controls[58]. These lasting changes in ELA-engaged PVT neurons may alter its output, a notion supported by our chemogenetic studies.

Distinct topological domains of the PVT contribute to sex-specific disruptions of reward behaviors

In adult mice, we tested whether the population of PVT neurons activated by, and therefore likely encoding, ELA is responsible for behavioral disruptions following ELA. In females, inhibition of ELA-engaged neurons in the posterior PVT ameliorated ELA-induced augmented consumption

of palatable food but produced no change in behavior in the control group. In contrast, inhibition of ELA-engaged neurons in the anterior PVT had no effect in the ELA group but decreased consumption in control females, recapitulating the ELA phenotype. Together, these results indicate a selective role for neurons engaged by ELA in the posterior PVT in ELA females' augmented reward behavior. They suggest that subpopulations of posterior PVT promote reward behaviors and further, that these subpopulations may be chronically overactive in adult ELA females. In ELA males, their anhedonia-like behaviors were consistent with minimal activity of engaged posterior PVT neurons. Accordingly, inhibition of these ELA-activated population in the posterior PVT had no effect on behavior

In contrast to the posterior PVT, ELA-engaged neurons in the anterior PVT seem to drive the anhedonia-like disruption of reward behaviors consequent to ELA in males. Thus, inhibition of ELA-engaged neurons in the anterior PVT of adult ELA males ameliorated their anhedonia-like phenotype. A similar 'anhedonia promoting' role for anterior PVT neurons engaged by salient early-life experiences in females emerges from our finding that inhibiting these neurons decreases reward seeking in females exposed to standard rearing.

Together, these findings identify for the first time that subpopulations of PVT neurons activated early in life contribute to either promoting (posterior PVT) or braking (anterior PVT) reward behaviors. Furthermore, the tonic level of their activity is modulated by adverse early-life experiences in a sex-dependent manner.

Finally, we define here the PVT as a brain hub encoding ELA. This takes place prior to the onset of an operational hippocampus-mediated memory system, which does not initiate until after the early sensitive period probed by our ELA model[59], leaving an explained window of time in early life during which experiences are somehow encoded. Given that experiences in the early

postnatal period can have profound impacts on emotional health in adulthood, a different brain region or regions must be responsible for encoding these experiences. Our studies point to the PVT, a brain region robustly and uniquely activated during ELA, as an important participant in this process.

In conclusion, the present studies indicate an important sex-dependent role for PVT neurons active during ELA in mediating enduring aberrant reward behaviors induced by this transient adverse experience. We identify new distinct and opposing roles for anterior and posterior PVT cell populations. We pinpoint the anterior PVT as a primary contributor to disrupted reward behaviors in adult males and the posterior PVT in females. suggesting intrinsic sex-dependent differences in the operations of the reward circuitry even prior to puberty.

Materials and Methods

Mice

Fos$^{tm2.1(icre/ERT2)Luo}$/J (Fos$^{2A\text{-}iCreER}$; Jax #030323), B6.129-Gt(ROSA)$^{26Sortm1(CAG\text{-}CHRM4*,\text{-}mCitrine)Ute}$/J (R26-LSL-Gi-DREADD; Jax #026219), B6N;129-Tg(CAG-CHRM3*,-mCitrine)1Ute/J (CAG-LSL-Gq-DREADD; Jax #026220), and B6.Cg-Gt(ROSA)26Sortm14(CAG-tdTomato)Hze/J (Ai14; Jax #007914) mice were obtained from The Jackson Laboratory or bred in house. All mice were housed in a temperature-controlled, quiet, and uncrowded facility on a 12-hour light/dark schedule (lights on at 7:00 AM, lights off at 7:00 PM) prior to cannula surgery. After surgery, mice were single-housed and maintained on a 12-hour reverse light cycle (lights on at midnight, lights off at noon) to enable behavioral testing during the dark-phase (active period); we have previously found no difference in any behavioral test between normally housed and reverse light cycle–housed mice when tested at the same point in their circadian cycle. Mice were provided with ad libitum access to water and a global soy protein-free extruded diet (2020X Teklad; Envigo). Progeny of Fos$^{2A\text{-}iCreER}$ mice bred with Ai14 reporter mice were used for immunohistochemistry

studies. Progeny of Fos$^{2A\text{-}iCreER}$ mice bred with R26-LSL-Gi-DREADD or CAG-LSL-Gq-DREADD mice were used for behavioral studies. All experiments were performed in accordance with National Institutes of Health guidelines and were approved by the University of California Irvine Institutional Animal Care and Use Committee.

Limited Bedding and Nesting (LBN) Model of Early Life Adversity (ELA)

Mouse dams were checked every morning for presence of copulatory plugs while paired with a male and placed into single housing on embryonic day (E)17, after which point the cage was checked for presence of pups every 12 hours. On the morning of postnatal day (P)2, litters were culled to a maximum of 8 (minimum of 4) including both sexes, and the ELA paradigm was initiated as previously described (Molet et al., 2014; Rice et al., 2008). Control dams and pups were placed in cages with a standard amount of corn cob bedding and one 5 x 5 cm cotton nestlet. ELA dams and pups were placed in a cage atop a fine-gauge plastic-coated aluminum mesh (cat #4700313244; McNichols Co., Tampa, FL) set approximately 2.5 cm above the cage floor, which was covered with a thin layer of corn cob bedding. ELA dams received one-half nestlet. All cages were placed in rooms with robust ventilation to avoid accumulation of ammonia. Both ELA and CTL dams and pups were left undisturbed until the afternoon of P6 (P5 for Fos$^{2A\text{-}iCreER}$ x CRFR1-flpO pups), at which point the pups were briefly removed from the home cage, placed in a new cage on a heating pad, and injected subcutaneously with 150 mg/kg tamoxifen (catalog no. T5648; MilliporeSigma) dissolved in corn oil (catalog no. C8267; MilliporeSigma) as previously described (Kooiker et al., 2023). Pups were then returned to their home cage and left undisturbed until the morning of P10. For Fos$^{2A\text{-}iCreER}$ x CRFR1-flpO pups only, individual pups were briefly removed from the home cage for a second time for ICV virus injection on P6. On the morning of P10, each pup was weighed, and the dam and pups were moved to standard cages, where maternal behaviors rapidly normalize and the ELA pups' stress dissipates. P5/6 was chosen as

the time point for tamoxifen injections because it is roughly at the midpoint of the ELA paradigm, allowing for optimal tagging of neurons activated by ELA rearing.

Cannula implantation surgery

P60 mice were anesthetized with 1-3% isoflurane and placed in a stereotactic frame. For intra-PVT drug infusions, a guide cannula (23G, 30G obturator) was implanted in the aPVT (AP: -0.4 mm; ML: mm; DV: mm) or pPVT (AP: -1.6 mm; ML: mm; DV: mm, 8° angle toward midline) and mounted to the skull with a screw and dental cement. Mice were given at least one week to recover before beginning behavioral experiments.

Chemogenetic studies

For excitatory (TRAP2 x CAG-LSL-Gq-DREADD mice) and inhibitory (TRAP2 x R26-LSL-Gi-DREADD) DREADD experiments, Clozapine-N-oxide (CNO) or vehicle (artificial cerebrospinal fluid, aCSF) were administered via microinfusion through an intra-PVT cannula. CNO (cat #HB6149, HelloBio, UK) was dissolved in aCSF at a concentration of 1 mM, and 0.2 µl of solution was administered at a rate of 50 nl/min. Microinjection needles were left in place for 2 min. following injection to allow for diffusion.

Behavioral assays

Behavioral assays were carried out in low light (<15 lux) and during the animal's active period. Prior to the start of testing, all mice were placed in the behavior room for at least 1 hr. to acclimate to their surroundings.

Palatable food consumption

Single-housed mice were habituated to ~1 g Cocoa Pebbles cereal in the home cage for 1 hr. on each of three days preceding the test day. On the test day, intra-PVT CNO or vehicle was administered 5 minutes prior to placing ~1 g pre-weighed Cocoa Pebbles into the cage. After 1 hr. or 1.5 hr., during which mice were left undisturbed, uneaten Cocoa Pebbles were collected

and weighed to determine consumption. Mice that never consumed >100 mg across all habituation and test days were excluded.

Sex cue preference test

For experiments in males, urine was collected from female mice in the estrous phase of their estrous cycle. Urine was collected on the same day as the test and was stored in capped 0.2 ml PCR tubes until use. 60 ul of urine and 60 ul of almond extract (a control, non-rewarding scent; Pure Almond extract, Target) were pipetted onto separate cotton swabs and affixed within opposite corners of the home cage of single-housed males. Intra-PVT CNO or vehicle were administered immediately before the test. During the test, mice were given free access to both swabs for 3 min. Time spent with the nose within 3 cm of each swab and locomotion were tracked using 3-point rodent tracking in Ethovision XT15 software (Noldus, US).

Brain processes and analysis

Following chemogenetic studies, mice were euthanized with sodium pentobarbital and transcardially perfused with ice cold phosphate-buffered saline (PBS) (pH = 7.4) followed by 4% paraformaldehyde in 0.1M sodium phosphate buffer (pH = 7.4). Perfused brains were postfixed in 4% paraformaldehyde in 0.1M PBS (pH= 7.4) for 12-16 hours before cryoprotection in 15%, followed by 30% sucrose in PBS. Brains were then frozen and coronally sectioned at a thickness of 25 um (1:5 series) using a LeicaCM1900 cryostat (Leica Microsystems). Sections were mounted on gelatin-coated slides and coverslipped with VECTASHIELD containing DAPI (catalog no. H-1200; Vector Laboratories).

For analyses following palatable food consumption, P60 $Fos^{2A\text{-}iCreER+/-}$::$Ai^{14+/-}$ mice were euthanized with sodium pentobarbital immediately following 90 min exposure to palatable food. Mice were then transcardially perfused with ice cold phosphate-buffered saline (PBS) (pH = 7.4) followed by 4% paraformaldehyde in 0.1M sodium phosphate buffer (pH = 7.4). Perfused brains

were postfixed in 4% paraformaldehyde in 0.1M PBS (pH= 7.4) for 12-16 hrs before cryoprotection in 15% sucrose in PBS, followed by 30% sucrose in PBS. Brains were then frozen and coronally sectioned at a thickness of 25 mm (1:5 series) using a LeicaCM1900 cryostat (Leica Microsystems). Following immunohistochemistry for cFos, Sections were mounted on gelatin-coated slides and coverslipped with VECTASHIELD containing DAPI (catalog no. H-1200; Vector Laboratories).

Immunohistochemistry

For fluorescent labeling of cFos following palatable food consumption, free-floating sections from P60 mice were first washed in PBS containing 0.3% Triton (PBST) (3 x 5 minutes), followed by incubation in 5% normal goat serum in PBST for 1 hr. at room temperature. Sections were then incubated with 1:10,000 rabbit anti-cFos antibody (Oncogene, Ab-5, PC38) diluted in 2% NGS in PBST for 2-3 days at 4°C. Following 3 x 5 min washes in PBST, sections were then incubated in 1:500 goat anti-rabbit 488 (cat #A-11008, Invitrogen, US) for 2 hrs. at room temperature. Sections were then washed 3 x 5 min in PBST, mounted on gelatin-coated slides, and coverslipped with Vectashield mounting medium with DAPI (Vectashield, Cat # H-1200, Vector Labs, US).

Image acquisition

Confocal images were collected using an LSM-510 confocal microscope (Zeiss) with an apochromatic 10X, 20X, or 63X objective. Virtual z sections of 1 mm were taken at 0.2- to 0.5-mm intervals. Image frame was digitized at 12-bit using a 1024 X 1024 pixel frame size.

Statistical analysis

tdT^+ and $cFos^+$ neuron numbers were counted manually in Fiji (Schindelin et al., 2012). All quantifications and analyses were performed using stereological principles including systematic unbiased sampling and without knowledge of group assignment. Statistical analyses were carried

out using GraphPad Prism (GraphPad Software). Differences between control and ELA groups of both sexes were assessed using two-way analysis of variance (ANOVA). To examine significance of cell number differences throughout the anteroposterior axis of the PVT, we used two-way mixed ANOVA with the Sidak multiple comparisons post hoc test.

Cross correlation analysis of brain regions activated during ELA or standard rearing

We counted the number of cells expressing the cFos reporter (activated or tagged) in brain regions with appreciable reporter expressing cells (Kooiker, 2023) and generated Pearson correlation coefficients for each pair of regions. To enable comparison of different animals we converted the correlations to z-scores and determined the difference between these scores in rearing groups (taking into account the number of observations within each rearing group for each pair). A stronger functional relationship between two regions in the ELA group is indicated by a positive Z_{obs} value and a red line, and a weaker functional relationship between two regions in the ELA group (and therefore a stronger relationship in control mice) is indicated by a negative Z_{obs} value and a blue line. Correlation coefficient differences between ELA and control groups for all regions are listed in **supplementary table 1**.

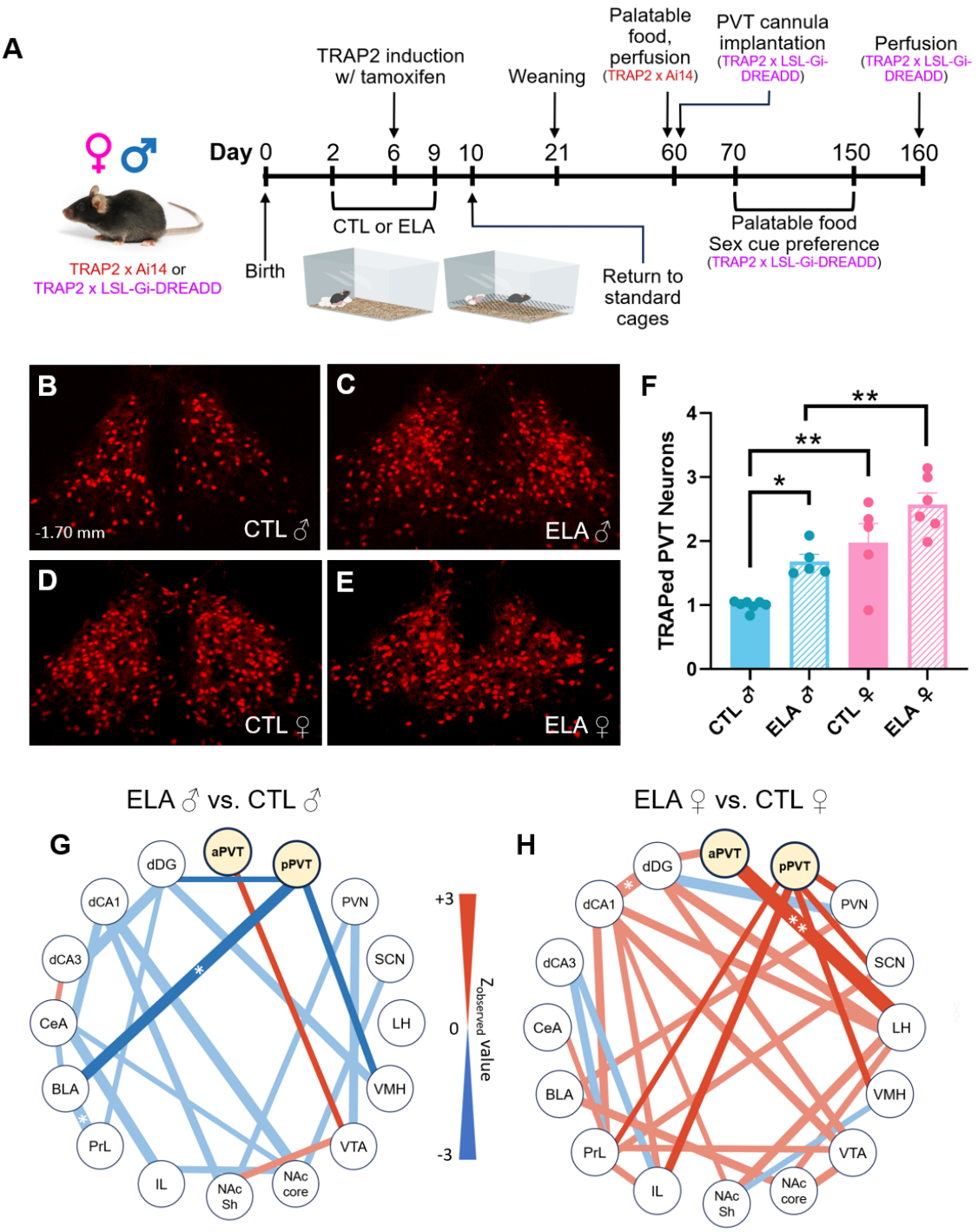

Figure 1. ELA-induced PVT and PVT network activation is sex-dependent (**A**) Experimental timeline of TRAP2 studies. (**B**) Representative images from male control and (**C**) ELA TRAP2 mice showing tdTomato reporter expression in the posterior PVT following TRAP induction with tamoxifen on P6. (**D**) Representative images from female control and (**E**) ELA TRAP2 mice

showing tdTomato reporter expression in the posterior PVT following TRAP induction with tamoxifen on P6. (**F**) Quantification of tdTomato$^+$ neurons in male and female control and ELA mice (*, $p < 0.05$; **, $p < 0.01$; n = 5-7 mice/group; 2-way mixed model ANOVA with Sidak *posthoc* test). Bars represent mean ± SEM. (**G**) Network connectivity map comparing correlated neuronal activity in ELA vs. control males. Red lines indicate greater a greater functional relationship between two regions in ELA males, and blue lines indicate a weaker functional relationship between two regions in ELA males. (*, $p < 0.05$) (**H**) Network connectivity map comparing correlated neuronal activity in ELA vs. control males. (*, $p < 0.05$; **, $p < 0.01$; CTL, control; ELA, early-life adversity; aPVT, anterior paraventricular nucleus of the thalamus; pPVT, posterior paraventricular nucleus of the thalamus; PVN, paraventricular nucleus of the hypothalamus; SCN, suprachiasmatic nucleus; LH, lateral hypothalamus; VMH, ventromedial hypothalamus; VTA, ventral tegmental area; NAc, nucleus accumbens; IL, infralimbic cortex; PrL, prelimbic cortex; BLA, basolateral amygdala; CeA, central amygdala; dCA3, dorsal hippocampus area CA3; dCA1, dorsal hippocampus area CA1; dDG, dorsal dentate gyrus).

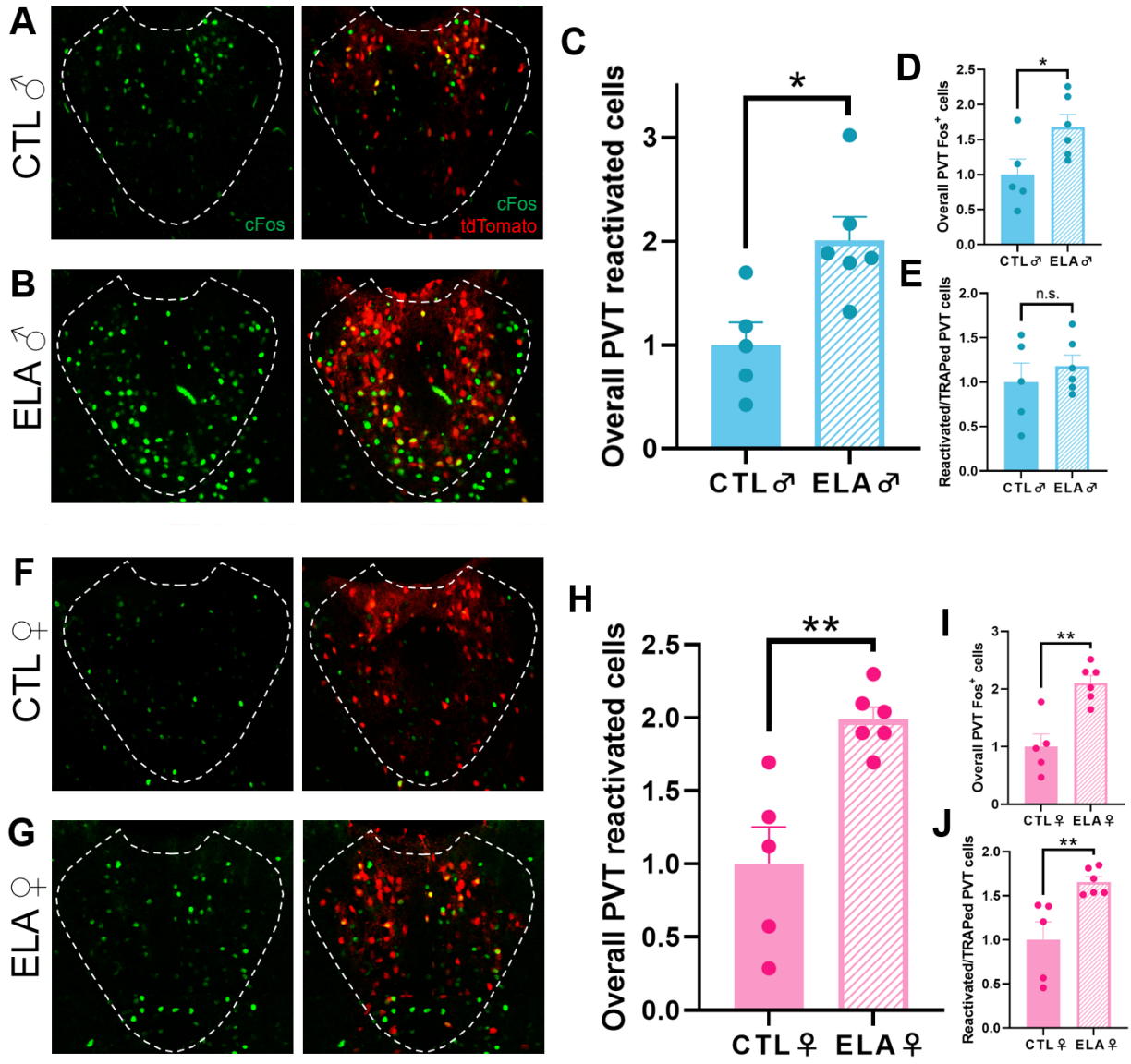

Figure 2. Reward-induced reactivation of early-life-engaged PVT neurons (**A**) Representative images in mid PVT of cFos expression and tdTomato co-expression in a control and (**B**) ELA male immediately following 1.5 hrs. of free access to palatable food. (**C**) Quantification of neurons co-expressing cFos and tdTomato across the PVT in P60 male control and ELA mice immediately following 1.5 hrs. of free access to palatable food ($p = 0.012$; n = 5-6 mice/group; Two-sided unpaired t-test). (**D**) Quantification of neurons expressing cFos across the PVT in male P60 control and ELA mice ($p = 0.038$; n = 5-6 mice/group; Two-sided unpaired t-test). (**E**) Proportion of tdTomato$^+$ PVT neurons co-expressing cFos in P60 control and ELA males

(p = 0.468; n = 5-6 mice/group; Two-sided unpaired t-test). (**F**) Representative images in mid PVT of cFos expression and tdTomato co-expression in a control and (**G**) ELA female immediately following 1.5 hrs. of free access to palatable food. (**H**) Quantification of neurons co-expressing cFos and tdTomato across the PVT in P60 female control and ELA mice immediately following 1.5 hrs. of free access to palatable food (p = 0.003; n = 5-6 mice/group; Two-sided unpaired t-test). (**I**) Quantification of neurons expressing cFos across the PVT in female P60 control and ELA mice (p = 0.002; n = 5-6 mice/group; Two-sided unpaired t-test). (**J**) Proportion of tdTomato$^+$ PVT neurons co-expressing cFos in P60 control and ELA females (p = 0.008; n = 5-6 mice/group; Two-sided unpaired t-test). Bars represent mean ± SEM.

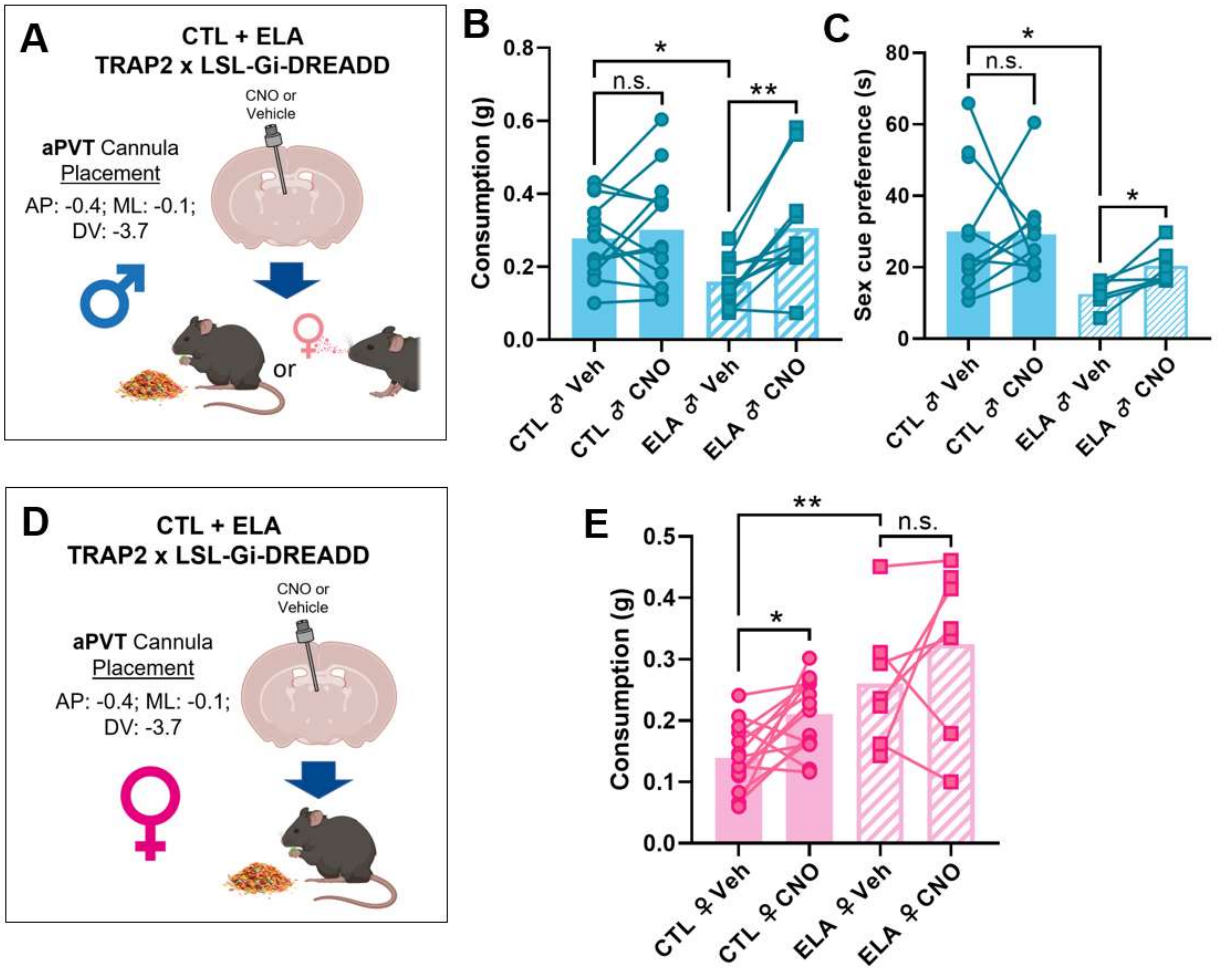

Figure 3. Inhibition of early-life-engaged anterior PVT neurons normalizes reward behaviors in adult ELA males. (**A**) Experimental schematic for aPVT inhibition in males. TRAP2 x LSL-Gi-DREADD mice received a tamoxifen injection on P6, inducing expression of an inhibitory DREADD in neurons active during ELA or standard rearing. A cannula for drug infusion was implanted in the aPVT of P60 mice and palatable food consumption and interest in a sex cue were measured following vehicle or CNO infusion. (**B**) Palatable food consumption following intra-aPVT vehicle or CNO microinfusion in control and ELA males (n = 9-13 mice/group; 2-way mixed model ANOVA with Sidak *post hoc* test). (**C**) Time spent sniffing estrous female urine in a 3 min. test following intra-aPVT vehicle or CNO microinfusion in control and ELA males. (n = 6-10

mice/group; 2-way mixed model ANOVA with Sidak *post hoc* test). (**D**) Experimental schematic for aPVT inhibition in females. (**E**) Palatable food consumption following intra-aPVT vehicle or CNO microinfusion in control and ELA females (n = 7-14 mice/group; 2-way mixed model ANOVA with Sidak *post hoc* test). *, $p < 0.05$; **, $p < 0.01$; n.s., not significant.

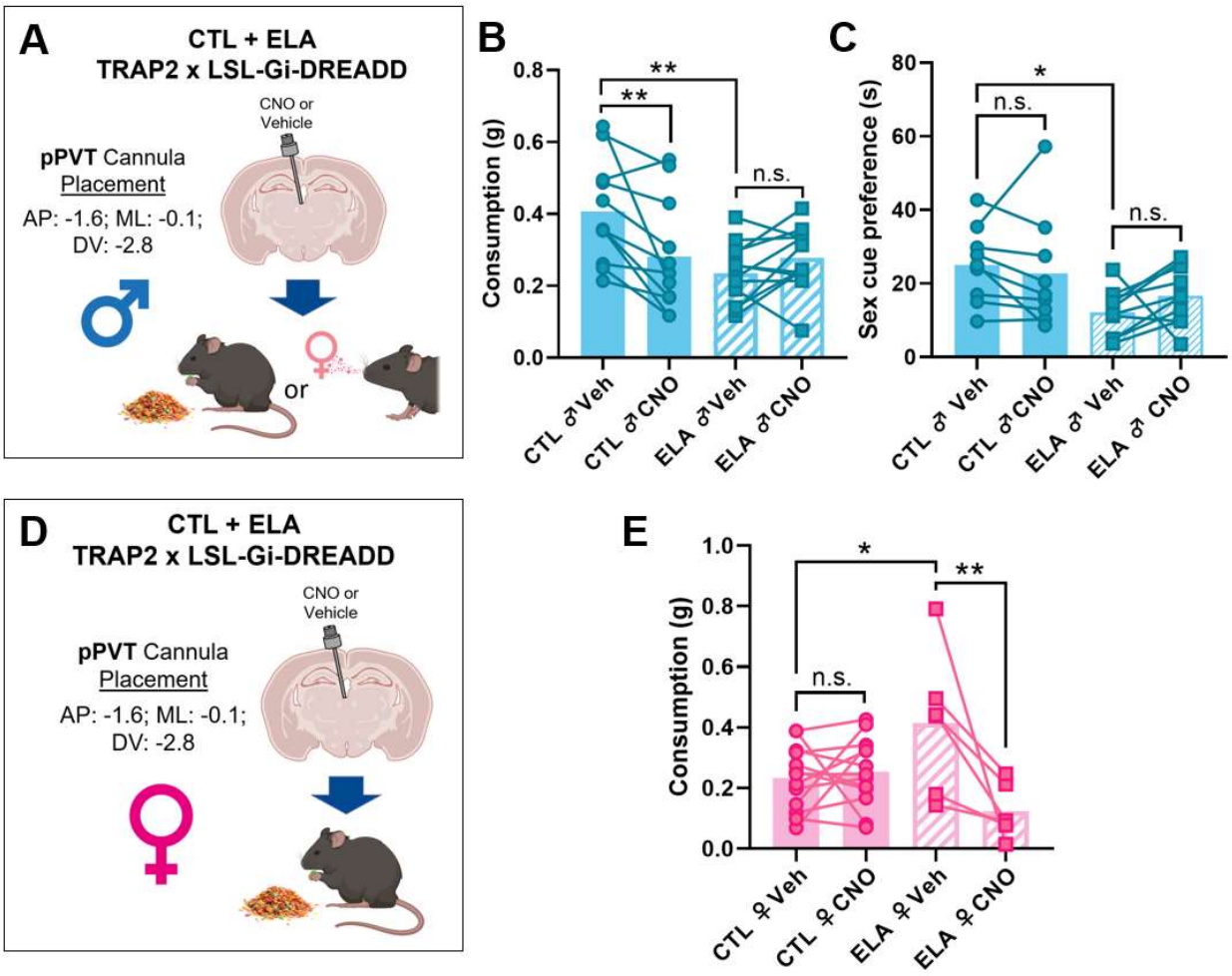

Figure 4. Inhibition of early-life-engaged posterior PVT neurons normalizes reward behaviors in adult ELA females. (**A**) Experimental schematic for pPVT inhibition in males. TRAP2 x LSL-Gi-DREADD mice received a tamoxifen injection on P6, inducing expression of an inhibitory DREADD in neurons active during ELA or standard rearing. A cannula for drug infusion was implanted in the pPVT of P60 mice and palatable food consumption was measured following vehicle or CNO infusion. (**B**) Palatable food consumption following intra-pPVT vehicle or CNO microinfusion in control and ELA males (n = 8-12 mice/group; 2-way mixed model ANOVA with Sidak *post hoc* test). (**C**) Time spent sniffing estrous female urine in a 3 min. test following intra-pPVT vehicle or CNO microinfusion in control and ELA males (n = 8-10 mice/group; 2-way mixed

model ANOVA with Sidak *post hoc* test). (**D**) Experimental schematic for pPVT inhibition in females. (**E**) Palatable food consumption following intra-pPVT vehicle or CNO microinfusion in control and ELA females (n = 6-10 mice/group; 2-way mixed model ANOVA with Sidak *post hoc* test).

References

1. American Psychiatric Association (2018): Stress in America Survey: Stress and Generation Z. Washington, DC: American Psychiatric Publishing.
2. Dube S. R. et al. Childhood abuse, neglect, and household dysfunction and the risk of illicit drug use: the adverse childhood experiences study. *Pediatrics*. **111**, 564–72 (2003).
3. Luby, J. L., Baram, T. Z., Rogers, C. E. & Barch, D. M. Neurodevelopmental optimization after early-life adversity: cross-species studies to elucidate sensitive periods and brain mechanisms to inform early intervention. *Trends Neurosci*. **43**, 744–751 (2020).
4. Short, A., & Baram, T. Z. Adverse early-life experiences and neurological disease: Age-old questions and novel answers. *Nat. Rev. Neurol.* **15**, 657–69 (2019).
5. Green, J. G. et al. Childhood adversities and adult psychiatric disorders in the national comorbidity survey replication I. *Arch. Gen. Psychiatry* 67, 113–123 (2010).
6. Boecker, R. et al. Impact of early life adversity on reward processing in young adults: EEG-fMRI results from a prospective study over 25 years. *PLoS One* **9**, e104185 (2014).
7. Callaghan, B. L., Sullivan, R. M., Howell, B., & Tottenham, N. The international society for developmental psychobiology Sackler symposium: Early adversity and the maturation of emotion circuits-A cross-species analysis. *Dev. Psychobiol*. **56**, 1635–1650 (2014).
8. Hanson, J. L., Hariri, A. R., & Williamson, D. E. Blunted ventral striatum development in adolescence reflects emotional neglect and predicts depressive symptoms. *Biol Psychiatry* **78**, 598–605 (2015).

9. McLaughlin, K. A., Weissman, D., & Bitran, D. Childhood Adversity and Neural Development: A Systematic Review. *Annu. Rev. Dev. Psychol*. **1**, 277–312 (2019).
10. Chen, Y., & Baram, T. Z. Toward understanding how early-life stress reprograms cognitive and emotional brain networks. *Neuropsychopharmacol.* **41**, 197–206 (2016).
11. Bolton, J. L. et al. Anhedonia following early-life adversity involves aberrant interaction of reward and anxiety circuits and is reversed by partial silencing of amygdala corticotropin-releasing hormone gene. *Biol Psychiatry* **83**, 137–147 (2018).
12. Goodwill, H. L. et al. Early life stress leads to sex differences in development of depressive-like outcomes in a mouse model. *Neuropsychopharmacol.* **44**, 711–720 (2019).
13. Levis, S. C. et al. Enduring disruption of reward and stress circuit activities by early-life adversity in male rats. *Transl. Psychiatry* **12**, 1–11 (2022).
14. Molet, J. et al. Fragmentation and high entropy of neonatal experience predict adolescent emotional outcome. *Transl. Psychiatry* **6**, e702 (2016).
15. Wakeford, A. G. P., Morin, E. L., Bramlett, S. N., Howell, L. L., & Sanchez, M. M. A review of nonhuman primate models of early life stress and adolescent drug abuse. *Neurobiol. Stress* **9**, 188–198 (2018).
16. Peña, C. J. et al. Early life stress confers lifelong stress susceptibility in mice via ventral tegmental area OTX2. *Science* **356**, 1185–1188 (2017).
17. Singh-Taylor, A. et al. NRSF-dependent epigenetic mechanisms contribute to programming of stress-sensitive neurons by neonatal experience, promoting resilience. *Mol. Psychiatry* **23**, 648–657 (2018).
18. Weaver, I. C. G. et al. Epigenetic programming by maternal behavior. *Nat. Neurosci*. **7**, 847–854 (2004).
19. Kooiker, C. L., Chen, Y., Birnie, M. T., & Baram, T. Z. Genetic Tagging Uncovers a Robust, Selective Activation of the Thalamic Paraventricular Nucleus by Adverse Experiences Early in Life. *Biol. Psychiatry Global Open Sci*. **3**, 746–755 (2023).

20. Fenoglio, K. A., Chen, Y., & Baram, T. Z. Neuroplasticity of the Hypothalamic-Pituitary-Adrenal Axis Early in Life Requires Recurrent Recruitment of Stress-Regulating Brain Regions. *J. Neurosci.* **26**, 2434–2442 (2006).
21. Barson, J. R., Mack, N. R., & Gao, W. J. The Paraventricular Nucleus of the Thalamus Is an Important Node in the Emotional Processing Network. *Front. Behav. Neurosci.* **14**, 1–9 (2020).
22. Iglesias, A. G., & Flagel, S. B. The Paraventricular Thalamus as a Critical Node of Motivated Behavior via the Hypothalamic-Thalamic-Striatal Circuit. *Front. Integr. Neurosci.* **15**, 1–10 (2021).
23. Penzo, M. A., & Gao, C. The paraventricular nucleus of the thalamus: an integrative node underlying homeostatic behavior. *Trends Neurosci*. **44**, 1–12 (2021).
24. Dong, X., Li, S., & Kirouac, G. J. Collateralization of projections from the paraventricular nucleus of the thalamus to the nucleus accumbens, bed nucleus of the stria terminalis, and central nucleus of the amygdala. *Brain Struct. Funct*. **222**, 3927–3943 (2017).
25. Li, S., & Kirouac, G. J. Projections From the Paraventricular Nucleus of the Thalamus to the Forebrain, With Special Emphasis on the Extended Amygdala. *J. Comp. Neurol.* **259**, 263–287 (2008).
26. Parsons, M., Li, S., & Kirouac, G. J. Functional and Anatomical Connection between the Paraventricular Nucleus of the Thalamus and Dopamine Fibers of the Nucleus Accumbens. *J. Comp. Neurol.* **259**, 1050–1063 (2007).
27. Vertes, R. P., & Hoover, W. B. Projections of the paraventricular and paratenial nuclei of the dorsal midline thalamus in the rat. *J. Comp. Neurol.* **508**, 212–237 (2008).
28. Bhatnagar, S., & Dallman, M. Neuroanatomical basis for facilitation of hypothalamic-pituitary- adrenal responses to a novel stressor after chronic stress. *Neurosci.*, **84**, 1025–1039 (1998).

29. Choi, E. A., & McNally, G. P. Paraventricular thalamus balances danger and reward. *J. Neurosci.* **37**, 3018–3029 (2017).

30. Choi, E. A., Jean-Richard-dit-Bressel, P., Clifford, C. W. G., & McNally, G. P. Paraventricular thalamus controls behavior during motivational conflict. *J. Neurosci.* **39**, 4945-4958 (2019).

31. Hsu, D. T., Kirouac, G. J., Zubieta, J.-K., & Bhatnagar, S. Contributions of the paraventricular thalamic nucleus in the regulation of stress, motivation, and mood. *Front. Behav. Neurosci.* **8**, 1–10 (2014).

32. Keyes, P. C. et al. Orchestrating Opiate-Associated Memories in Thalamic Circuits. *Neuron*, **107**, 1113-1123.e4 (2020).

33. Otis, J. M. et al. Prefrontal cortex output circuits guide reward seeking through divergent cue encoding. *Nature* **543**, 103–107 (2017).

34. Do-Monte, F. H., Quinõnes-Laracuente, K., & Quirk, G. J. A temporal shift in the circuits mediating retrieval of fear memory. *Nature* **519**, 460–463 (2015).

35. Penzo, M. A. et al. The paraventricular thalamus controls a central amygdala fear circuit. *Nature*, **519**, 455–459 (2015).

36. McNally, G. P. Motivational competition and the paraventricular thalamus. *Neurosci. Biobehav. Rev.* **125**, 193–207 (2021).

37. Zhu, Y. et al. Dynamic salience processing in paraventricular thalamus gates associative learning. *Science* **429**, 423–429 (2018).

38. DeNardo, L. A. et al. Temporal evolution of cortical ensembles promoting remote memory retrieval. *Nat. Neurosci.* **22**, 460–469 (2019).

39. Walker, C. D. et al. Chronic early life stress induced by limited bedding and nesting (LBN) material in rodents: critical considerations of methodology, outcomes and translational potential. *Stress* **20**, 421–448 (2017).

40. Birnie, M. T. et al. Stress-induced plasticity of a CRH/GABA projection disrupts reward behaviors in mice. *Nat. Commun.* **14**, 1–10 (2023).

41. Birnie, M. T. et al. Plasticity of the reward circuitry after early life adversity: mechanisms and significance. *Biol. Psychiatry* **87**, 1–10 (2020).

42. Levis, S. C. et al. On the early life origins of vulnerability to opioid addiction. *Mol. Psychiatry* **26**, 4409-4416 (2019).

43. Machado, T. et al. Early life stress is associated with anxiety, increased stress responsivity and preference for “comfort foods” in adult female rats. *Stress* **16**, 549–556 (2013).

44. Parks, B. J. et al. Limited bedding and nesting increases ethanol drinking in female rats. *Pharmacol. Biochem. Behav.* **239**, 173756 (2024).

45. Curtis, G. R., Oakes, K., & Barson, J. R. Expression and Distribution of Neuropeptide-Expressing Cells Throughout the Rodent Paraventricular Nucleus of the Thalamus. *Front. Behav. Neurosci.* **14**, 1–14 (2021).

46. Gao, C. et al. Two genetically, anatomically and functionally distinct cell types segregate across anteroposterior axis of paraventricular thalamus. *Nat. Neurosci.* **23**, 217-228 (2020).

47. Li, S., & Kirouac, G. J. Sources of inputs to the anterior and posterior aspects of the paraventricular nucleus of the thalamus. *Brain Struct. Funct*. **217**, 257–273 (2012).

48. Shima, Y. et al. Distinctiveness and continuity in transcriptome and connectivity in the anterior-posterior axis of the paraventricular nucleus of the thalamus. *Cell Rep.* **42**, 113309 (2023).

49. Malkesman, O. et al. The female urine sniffing test: a novel approach for assessing reward-seeking behavior in rodents. *Biol. Psychiatry* **67**, 864–871 (2010).

50. Roberts, S. A., Mclean, L. & Beynon, R. Darcin: a male pheromone that stimulates female memory and sexual attraction to an individual male’s odour. *Artic. BMC Biol*. **8**, 75 (2010).

51. McGaugh J. L. The amygdala modulates the consolidation of memories of emotionally arousing experiences. *Annu. Rev. Neurosci.* **27**, 1–28 (2004).

52. Sengupta, A. et al. Basolateral amygdala neurons maintain aversive emotional salience. J. *Neurosci*. **38**, 3001–3012 (2018).

53. Li, H. et al. Neurotensin orchestrates valence assignment in the amygdala. *Nature* **608**, 586-592 (2022).

54. Tang, Q. Q. et al. Direct paraventricular thalamus-basolateral amygdala circuit modulates neuropathic pain and emotional anxiety. *Neuropsychopharmacol.* **49**, 455–466 (2024).

55. Haight, J. L. et al. The lateral hypothalamus and orexinergic transmission in the paraventricular thalamus promote the attribution of incentive salience to reward-associated cues. *Psychopharmacol.* **237**, 3741–3758 (2020).

56. Kirouac, G. J., Parsons, M. P., & Li, S. Orexin (hypocretin) innervation of the paraventricular nucleus of the thalamus. *Brain Res.* **1059**, 179–188 (2005).

57. Mátyás, F. et al. A highly collateralized thalamic cell type with arousal-predicting activity serves as a key hub for graded state transitions in the forebrain. *Nat. Neurosci.* **21**, 1551–1562 (2018).

58. Floriou-Servou, A. et al. A double TRAP reveals the influence of early life adversity on the translatome of the paraventricular nucleus of the thalamus (PVT) [Poster abstract]. Society for Neuroscience, Washington, D.C., United States (2023).

59. Donato, F. et al. The ontogeny of hippocampus-dependent memories. *J. Neurosci.* **41**, 920–926 (2021).

Acknowledgements

This work was supported by National Institute of Health grants RO1 MH132680 (M.T.B. T.Z.B.), F30 MH126615 (C.L.K.), T32 DA050558 (C.L.K.), T32 GM008620 (C.L.K.), and P50 MH096889 (M.T.B., T.Z.B.).

We thank Graciella Angeles, Amber Aourangzeb, and Mackenzie Morrison for technical assistance.

Author contributions

C.L.K., M.T.B., and T.Z.B. contributed to study design. C.L.K., Q.D., and N.T., contributed to data collection. C.L.K. conducted all surgeries. C.L.K., Q.D., and N.T. conducted all behavior studies. C.L.K and N.T. conducted histological analyses. C.L.K. and T.Z.B. wrote the paper. All authors discussed and commented on the manuscript.

Competing interests statement

The authors report no biomedical financial interests or potential conflicts of interest.

Supplementary Figures

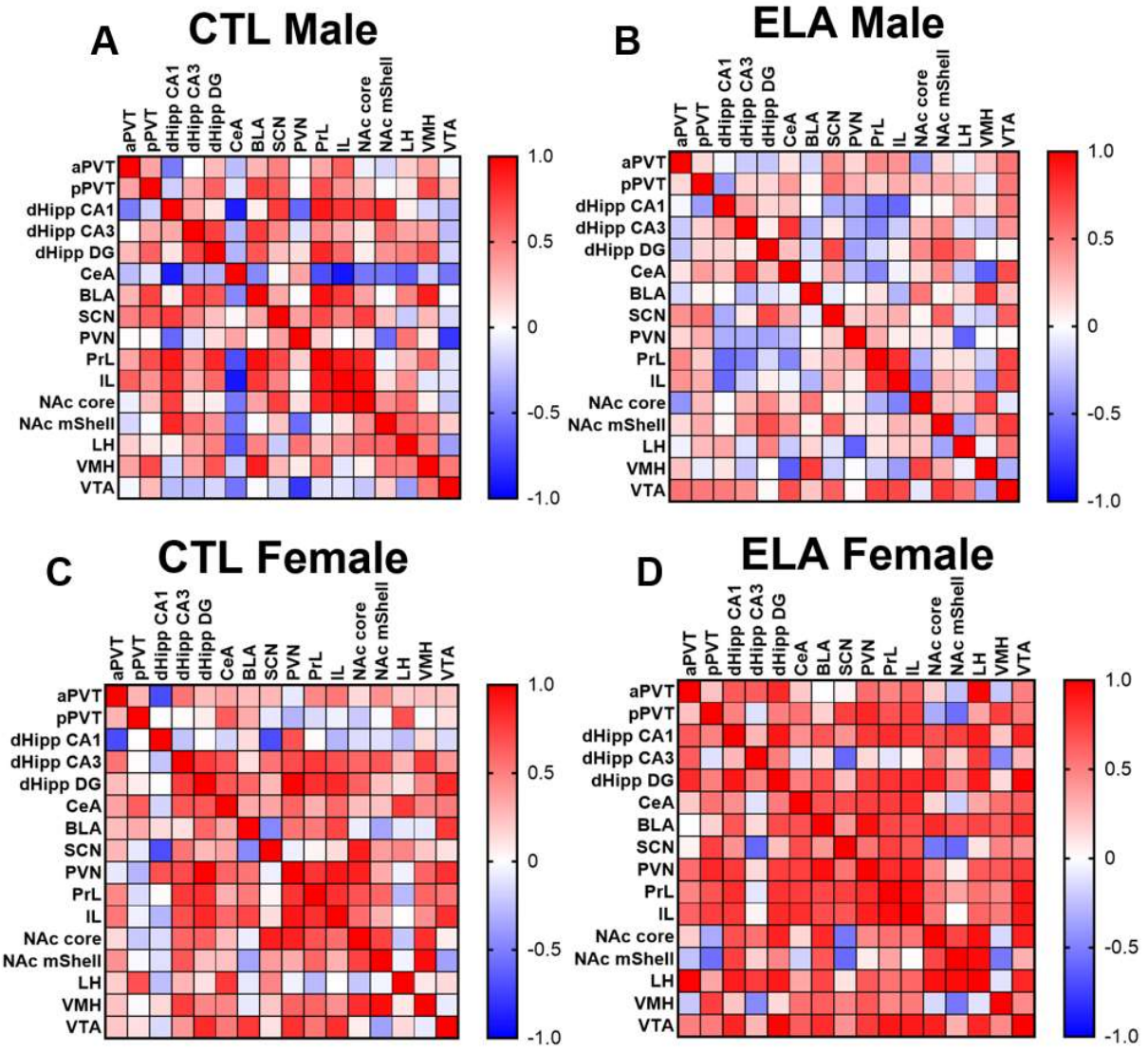

Supplementary Figure 1. Correlated neuronal activity between salient brain regions. Functional connectivity during ELA or standard rearing was assessed by computing Pearson correlations of normalized counts of cFos^{+} cells among the indicated brain regions. Correlation matrices were computed for (**A**) control males, (**B**) ELA males, (**C**) control females, and (**D**) ELA females. Red squares indicate a positive correlational relationship in activity between two regions while blue squares indicate a negative relationship.

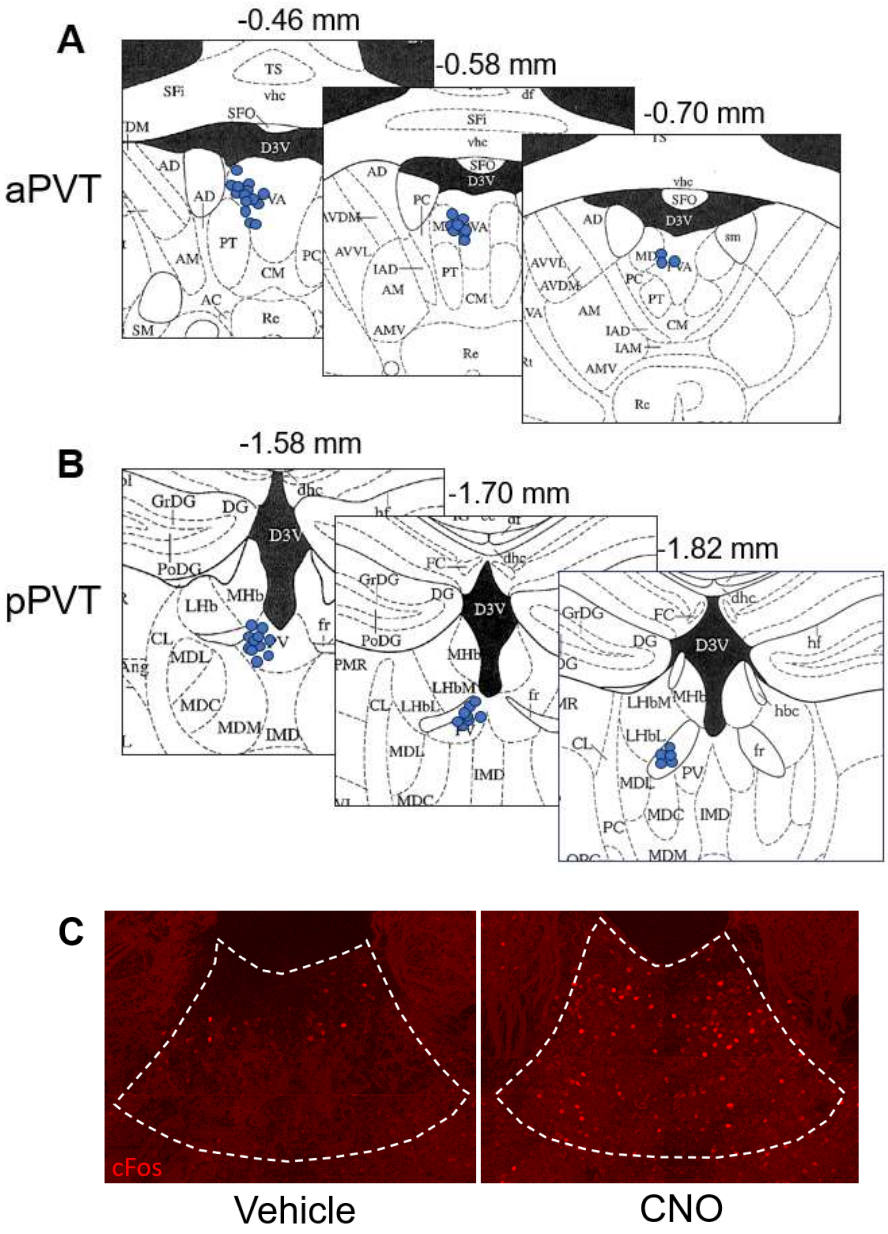

Supplementary Figure 2. PVT cannula locations for DREADD experiments (**A**) Terminal points of intra-aPVT drug infusion cannulas at three points along the rostrocaudal axis (shown as mm from Bregma). (**B**) Terminal points of intra-pPVT drug infusion cannulas at three points along the rostrocaudal axis (shown as mm from Bregma). (**C**) PVT cFos expression following intra-PVT vehicle or CNO infusion in mice with TRAP2-mediated Gq-DREADD expression

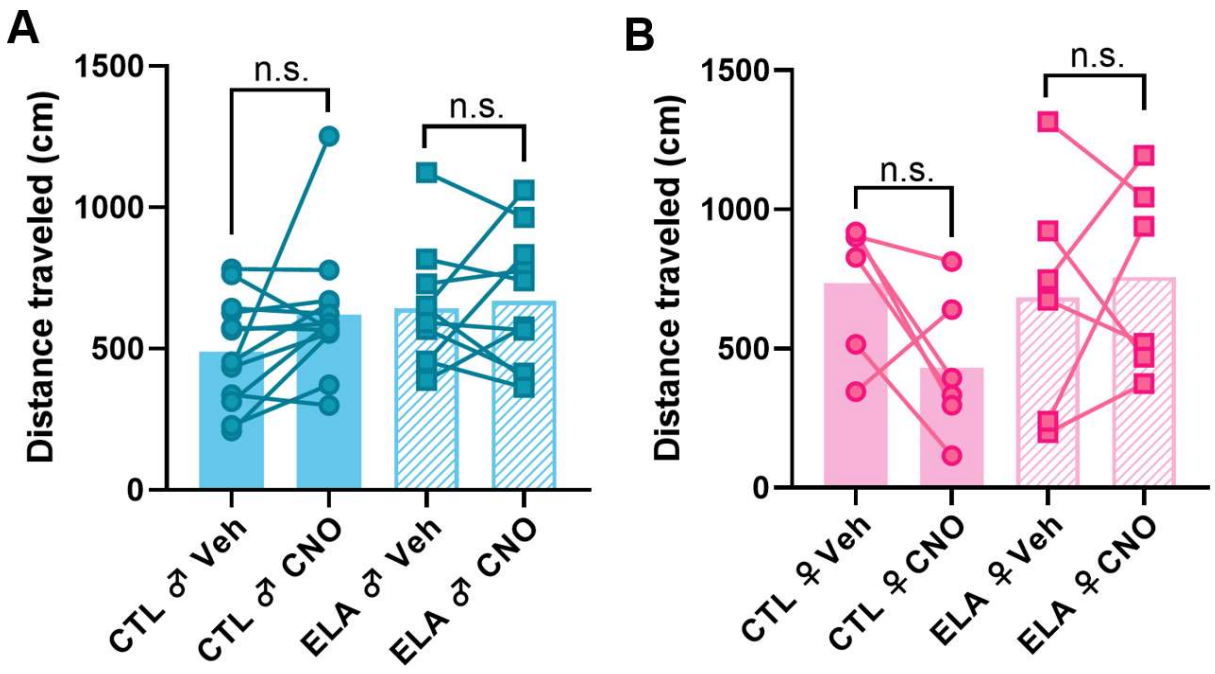

Supplementary Figure 3. Intra-PVT CNO infusion and rearing do not influence locomotion. (**A**) Neither ELA nor intra-PVT CNO microinfusion influence locomotion over the course of 3 minutes in males (n = 10-12 mice/group) (**B**) or females (n = 6 mice/group).

Male Z_{obs} (ELA-CTL)	aPVT	pPVT	dHipp CA1	dHipp CA3	dHipp DG	CeA	BLA	SCN	PVN	PrL	IL	NAc core	NAc mShell	LH	VMH	VTA
aPVT		-0.533	-0.989	0.368	-0.090	-0.314	-0.272	-0.141	0.311	0.214	-0.413	0.724	-0.017	-0.212	-0.222	1.038
pPVT	-0.533		0.385	-0.320	-1.017	0.661	-1.992	-0.264	0.654	-0.980	-0.205	0.033	0.648	0.296	-1.336	0.538
dHipp CA1	-0.989	0.385		0.052	0.127	-1.545	-0.069	-0.634	-0.334	-0.760	-0.392	-1.222	-1.511	0.586	-0.107	0.421
dHipp CA3	0.368	-0.320	0.052		-1.930	1.020	-0.940	-0.393	0.205	0.026	-0.108	0.251	-0.224	-0.457	-0.335	0.261
dHipp DG	-0.090	-1.017	0.127	-1.930		-0.065	-0.858	0.595	0.229	-1.025	-0.585	0.559	0.516	-0.010	-1.548	-0.212
CeA	-0.314	0.661	-1.545	1.020	-0.065		-1.054	0.741	-0.229	-0.440	-1.896	-1.000	-0.307	-0.656	0.652	0.381
BLA	-0.272	-1.992	-0.069	-0.940	-0.858	-1.054		-0.603	-0.025	-2.037	-0.931	0.465	0.043	-0.417	-0.473	0.340
SCN	-0.141	-0.264	-0.634	-0.393	0.595	0.741	-0.603		-0.448	-0.761	-0.274	-1.867	0.912	-0.087	-0.072	0.853
PVN	0.311	0.654	-0.334	0.205	0.229	-0.229	-0.025	-0.448		0.181	0.080	-0.065	-1.129	0.101	-0.062	-1.548
PrL	0.214	-0.980	-0.760	0.026	-1.025	-0.440	-2.037	-0.761	0.181		-0.510	-0.890	0.060	-0.139	-0.427	0.675
IL	-0.413	-0.205	-0.392	-0.108	-0.585	-1.896	-0.931	-0.274	0.080	-0.510		-1.224	0.169	-0.241	0.279	0.639
NAc core	0.724	0.033	-1.222	0.251	0.559	-1.000	0.465	-1.867	-0.065	-0.890	-1.224		-0.484	-0.507	0.983	-0.209
NAc mShell	-0.017	0.648	-1.511	-0.224	0.516	-0.307	0.043	0.912	-1.129	0.060	0.169	-0.484		-0.350	-0.272	1.261
LH	-0.212	0.296	0.586	-0.457	-0.010	-0.656	-0.417	-0.087	0.101	-0.139	-0.241	-0.507	-0.350		-0.939	0.289
VMH	-0.222	-1.336	-0.107	-0.335	-1.548	0.652	-0.473	-0.072	-0.062	-0.427	0.279	0.983	-0.272	-0.939		-0.374
VTA	1.038	0.538	0.421	0.261	-0.212	0.381	0.340	0.853	-1.548	0.675	0.639	-0.209	1.261	0.289	-0.374	

Female Z_{obs} (ELA-CTL)	aPVT	pPVT	dHipp CA1	dHipp CA3	dHipp DG	CeA	BLA	SCN	PVN	PrL	IL	NAc core	NAc mShell	LH	VMH	VTA
aPVT		-0.082	-0.164	0.231	1.447	-0.251	-0.377	-0.300	0.607	0.040	0.183	0.065	-0.288	2.592	-0.018	0.427
pPVT	-0.082		0.880	0.185	0.792	-0.196	-0.248	1.140	1.067	1.099	1.521	0.176	0.833	-0.611	1.253	0.630
dHipp CA1	-0.164	0.880		0.079	2.475	0.448	0.934	-0.544	0.254	1.885	1.215	0.845	1.031	1.477	0.099	1.479
dHipp CA3	0.231	0.185	0.079		-0.761	-1.000	0.034	0.107	-0.841	-1.532	-1.308	-0.087	-0.731	0.925	-0.618	-0.186
dHipp DG	1.447	0.792	2.475	-0.761		-0.339	0.280	-0.039	-1.937	-0.065	-0.044	0.733	0.325	1.739	-0.479	1.428
CeA	-0.251	-0.196	0.448	-1.000	-0.339		0.745	0.654	0.334	0.999	0.685	-0.146	-0.084	-0.893	0.153	0.244
BLA	-0.377	-0.248	0.934	0.034	0.280	0.745		-0.094	1.271	0.456	-0.056	1.468	0.559	0.961	0.757	0.159
SCN	-0.300	1.140	-0.544	0.107	-0.039	0.654	-0.094		0.636	1.207	0.873	-0.795	0.266	-0.493	0.361	0.369
PVN	0.607	1.067	0.254	-0.841	-1.937	0.334	1.271	0.636		0.077	-0.251	-0.678	-0.220	0.786	0.073	-0.085
PrL	0.040	1.099	1.885	-1.532	-0.065	0.999	0.456	1.207	0.077		1.204	-0.227	-0.379	0.442	-0.256	1.160
IL	0.183	1.521	1.215	-1.308	-0.044	0.685	-0.056	0.873	-0.251	1.204		-0.051	-0.370	0.893	0.141	0.434
NAc core	0.065	0.176	0.845	-0.087	0.733	-0.146	1.468	-0.795	-0.678	-0.227	-0.051		-0.052	1.265	-0.858	1.412
NAc mShell	-0.288	0.833	1.031	-0.731	0.325	-0.084	0.559	0.266	-0.220	-0.379	-0.370	-0.052		1.592	-1.114	-0.081
LH	2.592	-0.611	1.477	0.925	1.739	-0.893	0.961	-0.493	0.786	0.442	0.893	1.265	1.592		0.029	0.986
VMH	-0.018	1.253	0.099	-0.618	-0.479	0.153	0.757	0.361	0.073	-0.256	0.141	-0.858	-1.114	0.029		0.368
VTA	0.427	0.630	1.479	-0.186	1.428	0.244	0.159	0.369	-0.085	1.160	0.434	1.412	-0.081	0.986	0.368	

Supplementary Table 1. Difference between correlation coefficients in ELA vs. control males and ELA vs. control females